Revue Roumaine de Chimie, **2008**, *53*(12), 1105–1115

METHANE COMBUSTION OVER A COMMERCIAL PLATINUM ON ALUMINA CATALYST: KINETICS AND CATALYST DEACTIVATION

Magdalena BOŞOMOIU, Grigore BOZGA* and Gheorghe SOARE

Department of Chemical Engineering, Faculty of Applied Chemistry and Materials Science, University "Politehnica" of Bucharest, Polizu street no. 1 Bucharest, 011061, Roumanie

Received May 5, 2008

The aim of this study was to investigate the process of catalytic methane combustion in air over commercial platinum on alumina catalyst. Experiments were performed with methane concentrations in air between 0.6 % and 2.2 % (mol) and space velocities on the interval 15000 $cm^3/(g_{cat}\ h)$ to 60000 $cm^3/(g_{cat}\ h)$. The investigations of the process kinetics evidenced a good adequacy of the first order power law model for lean methane mixture combustion data. During the combustion experiments, it was observed a significant deactivation of the catalyst, particularly on first 25-30 hours of running. A deactivation experiment in isothermal conditions at 605 ^oC was carried out, this evidencing an approximately 50 % decrease of catalyst activity on the first 50 hours of on stream time. On the following time interval the rate of deactivation becomes much smaller, appearing a trend of stabilization. An empirical relation was also proposed in order to describe the time dependence of catalyst activity.

INTRODUCTION

Catalytic combustion is one of the technologies suitable for the treatment of gaseous effluents containing volatile organic compounds (VOC) at low concentration levels characteristic for commercial activities (usually less than 1000 ppm). The main advantages of this method concern the total combustion to CO_2 (low CO emissions) and lower NO_x emissions due to a lower process temperature compared to non-catalytic combustion technologies. Besides the catalytic activity, an important quality of a catalyst usable for commercial VOC combustion applications has to be a good resistance to deactivation, *i.e.* maintaining a minimum level of activity over sufficiently long time intervals, by avoiding excessive sintering or poisoning in the process environment. The sintering resistance and chemical stability of catalytically active phases is a key technical problem that must be solved for the development of commercially viable combustion catalysts. As pointed-out by Cordonna *et al.*,[1] a commercial combustion catalyst must operate without replacement for 20,000 hours or more, in the temperature range 250 to 650^{o}C.

Noble metals have been extensively studied and several reviews about their catalytic activity, mechanism of combustion and deactivation have been published.[2-6] One of the most widely used catalysts for control of many types of gaseous pollutants is platinum on alumina.[7-10] It is well known that in the presence of oxygen, platinum oxidizes into PtO_2 highly unstable compared to PdO formed in the case of Pd based catalysts (PtO_2 decomposes at a much lower temperature, around 400 ^{o}C). In addition, PtO_2 is highly volatile and this property is often considered to explain reconstruction of platinum surfaces under oxygen atmosphere by transport of Pt in the form of PtO_2 over nanometric distances. Generally palladium is more active in the oxidized state and consequently is preferred for operation at net-oxidizing (fuel lean) conditions, whereas Pt, which is more active in the metallic state, may be beneficial for net-reducing (fuel rich) conditions.[11-14]

Among the hydrocarbons, methane is the most resistant to oxidation, as reflected by the relatively high temperatures required to carry on the combustion process. From a mechanistic standpoint, the low reactivity of methane is connected to the symmetry of its molecule and the difficulty in which adsorption occurs on different

* Corresponding author: tel.:+40 21 4023883; fax: +40 21 3185900; e-mail address: g_bozga@chim.upb.ro

catalytic surfaces, when is compared with higher alkanes.[15] Trimm and Lam,[16] assumed that the permanent deactivation of platinum on alumina catalysts used in methane combustion was due to sintering of platinum or of alumina, the latter effect being accelerated in the presence of steam.

In this work we studied the methane combustion in air over a commercial Pt/Al_2O_3 (Engelhard commercial catalyst ESCAT 26 with 0.5% wt. Pt) at gas space velocities (GHSV) between 15000 and 60000 $cm^3/(g_{cat} \cdot h)$ and feed methane concentrations in air of 0.6 to 2.2 mole %. To describe the combustion kinetics we tested on our data the main published kinetic models for this process. The results evidenced that, due to the high oxygen excess, all the proposed kinetic expressions can be reduced to a first order dependence in respect with methane concentration. A deactivation experiment was also conducted in isothermal conditions at 605°C and atmospheric pressure.

EXPERIMENTAL PART

Catalyst characterization

Before use, the commercial catalyst grains were crushed and sieved in order to limit the influence of internal diffusion. The catalyst was then characterized by SEM, EDAX, specific surface area (BET), pore size distribution (BJH method on Autosorb-1 Quantachrome apparatus) and pellet size distribution (Table 1).

In order to identify the catalyst grain size free of internal diffusion influence, preliminary combustion experiments were carried out with different classes of grain dimensions, in identical working conditions, on the high temperature and flow rate domains. The results are presented in Fig. 1. As seen from this diagram, practically the influence of the internal diffusion can be neglected for particle dimensions smaller than 250 μm. All the following described experiments were performed on this class of particles. The grain size distribution (measured by X ray diffraction method on a Mastersizer Hydro 2000S instrument) is laying on the interval 50 – 250 μm and corresponds to an average dimension of 74.7 μm.

Table 1

Physical characteristics of the used Pt/Al_2O_3 catalyst

Parameter	Value
Bulk density	0.65 g/cm^3
Specific surface area (BET)	97.02 m^2/g
Range of pores size	50 to 250 Å
Mean pore diameter	236 Å

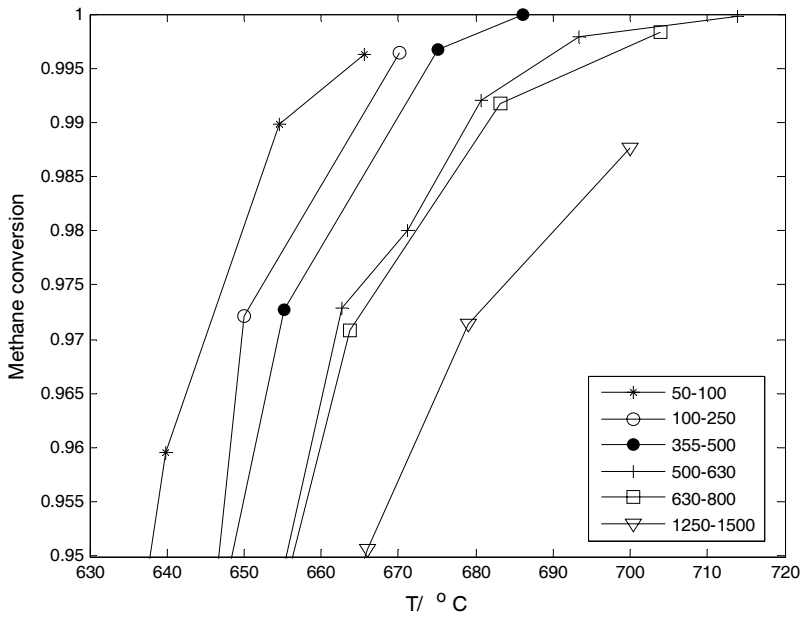

Fig. 1 – Experimental study of the internal diffusion influence for methane combustion over Pt/Al_2O_3 catalyst.

Experimental tests

The experimental setup used in the catalytic combustion study is depicted in Fig. 2. Approximately 0.2 g catalyst powder was loaded in a quartz tube reactor (i.d. = 4 mm) between two layers of quartz beads to assure uniform gas flow in the catalyst bed. The quartz tube was placed in a furnace provided with temperature controller.

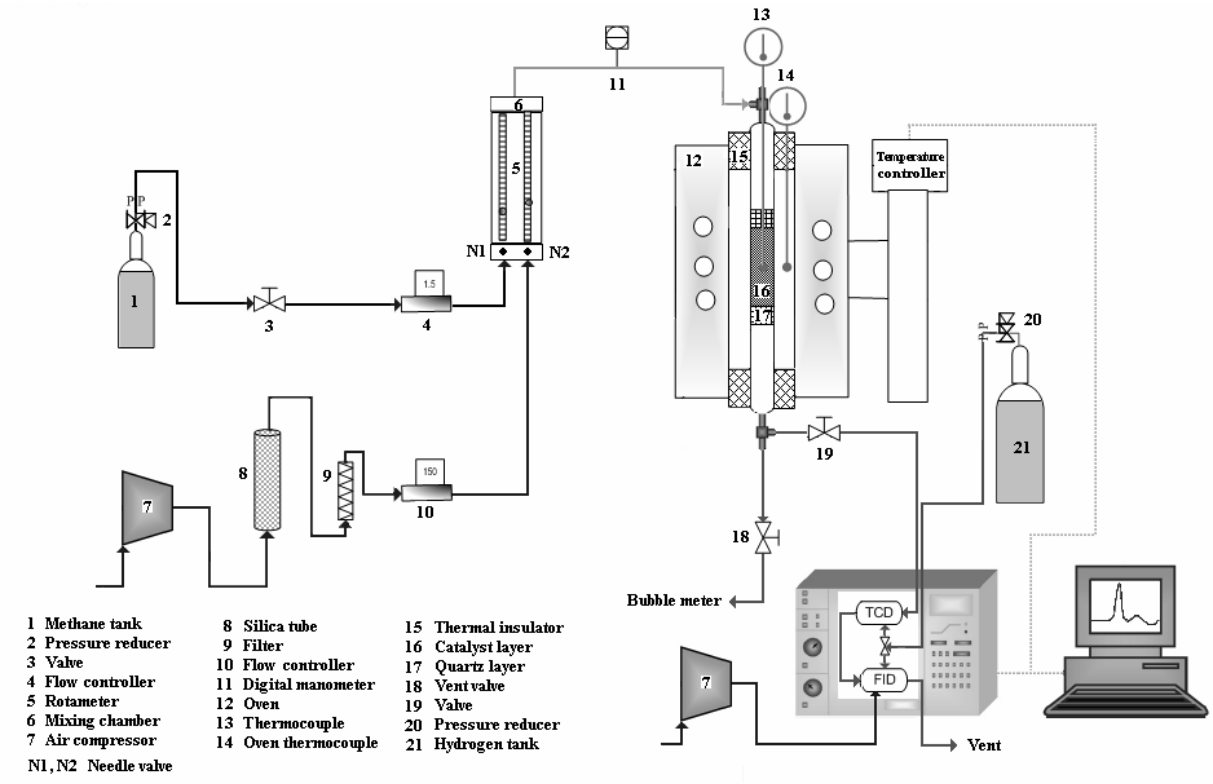

Fig. 2 – Schematic diagram of the experimental set-up for methane catalytic combustion.

The reaction temperature was monitored at the centre of the catalyst bed with a Pt/Rh thermocouple having the accuracy of 0.1 °C. The methane combustion was performed by oxygen from air. The gaseous mixture of methane and air was fed into reactor at flow rates varying in the range of 1500-12000 cm^3 h^{-1} and various methane concentrations (0.6, 1.2 and 2.2 mol %). The air and methane flow rates were measured and regulated by electronic Dwyer ™ controllers. The products concentrations in the reactor effluent were measured on-line by gas chromatography, using a Varian CP-3800 GC equipped with methanizer, FID and TCD detectors. A molecular sieve 5Å column and a Hayesep Q column, were used for N_2, O_2, CO and CH_4, respectively for CO_2 analysis. The calibration of the composition analyzer was performed by using analytical etalon mixtures. The pressure drop in the reactor was always lower than 0.2 bar, thus it was considered that experiments were conducted at atmospheric pressure. Before the combustion tests, the catalyst was activated and stabilized for two hours at 600 °C under reaction conditions.[17] The methane conversion was calculated from the concentration measurements of methane and carbon oxides at the inlet and the outlet of the reactor. The consistency of the measured data was checked by calculating the carbon balance around the reactor, having inlet and outlet flow rates and concentration measurements of carbon compounds. The carbon balance evidenced errors smaller than 5% for all the experiments.

RESULTS AND DISCUSSION

In order to check the level of catalytic activity of other solid surfaces present along the Pt/alumina in the reaction medium (stainless steel thermocouple wall and the quartz) we performed two combustion tests in the absence and presence of Pt/alumina. The results, presented in Fig. 3, show that in the absence of the Pt/alumina, the measured conversion temperature curve is practically superposed on a homogeneous combustion curve published in literature.[18] The values of reaction temperature corresponding to 10%, 50% and 99% methane conversions (T_{10}, T_{50} and T_{99}) in the presence of Pt/Al_2O_3 and in its absence (thermal combustion) are compared in Table 2. Consequently, it can be concluded that the catalytic effects of the thermowell surface and of quartz beads are negligible. The composition measurements showed that, practically, in all the catalytic combustion experiments water and carbon dioxide were the only products.

Table 2

Pt/Al_2O_3 activity in methane combustion as compared with thermal combustion
(1.2 % CH_4; 3000 cm^3/h; 0.2 g of catalyst; catalyst particle size 50-100 μm)

	T_{10} / (°C)	T_{50} / (°C)	T_{99} / (°C)
Pt/Al_2O_3	455	550	628
Thermal combustion	804	822	873

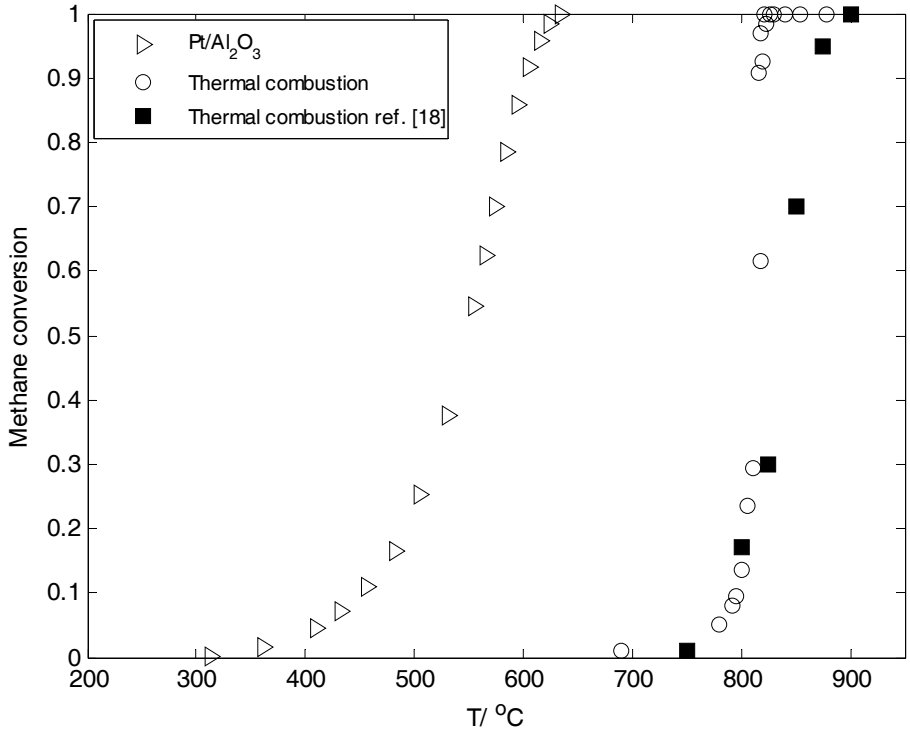

Fig. 3 – Methane conversion vs. temperature (1.2 mole % CH_4, total flow rate 3000 cm^3/h; 0.2 g catalyst; particle size 50-100 μm).

To check the influence of the gas–solid mass transfer step, we evaluated the external dimensionless concentration gradient of methane for each class of particles. The methane mass flux transferred toward the external catalyst surface, including diffusion and convection contributions can be calculated by the expressions:[19, 20]

$$N_A = \frac{k_G C_t}{f_A}(y_A - y_{A,S}) \; ; \quad f_A = 1 + \delta_A \bar{y}_A \; ; \quad \bar{y}_A = (y_{A,S} + y_A)/2; \quad \delta_A = \frac{\Delta v}{v_A} \tag{1}$$

Because the predominant reaction is the combustion to CO_2 and the value of $\bar{y}_A$ is very small (due to the air excess) f_A was approximated to one. The methane balance on the volume unit of catalyst bed is expressed by the equation:

$$a_v \; k_G \; C_t \; (y_A - y_{A,S}) = r_{A,S} \quad ; \quad r_{A,S} = k_m \; p \; y_{A,S} \; \rho_{bed} \tag{2}$$

The gas–solid mass transfer coefficient was evaluated from the equation proposed by Yoshida *et al.*:[21]

$$j_D = \frac{k_G}{u} \cdot Sc^{2/3} = 0.84 \, Re_p^{-0.51} \quad ; \quad Re_p = \frac{u \; \rho}{0.9 \; a_v \; \eta} \; ; \quad a_v = \frac{6 \cdot (1-\varepsilon)}{d_p} \; ; \quad Sc = \frac{\eta}{\rho D_A} \tag{3}$$

Assuming ideal behaviour of the reaction mixture and a first order reaction kinetics in respect with methane, one obtains the following global combustion rate expression:

$$r_{A,S} = K \rho_{bed} \; C_A \quad ; \quad \frac{1}{K} = \frac{1}{k_m RT} + \frac{\rho_{bed}}{k_G a_v} ; \; C_A = C_t \, y_A \tag{4}$$

In this expression, $\frac{1}{K}$ can be considered as the overall resistance opposed to the combustion process by the surface steps (first term) and external mass transfer respectively (second term). The external dimensionless concentration gradient of methane, equal to the weight of the resistance opposed by external mass transfer, is given by the expression:

$$\frac{y_A - y_{A,S}}{y_A} = \frac{K\,\rho_{bed}}{k_G\,a_v} \tag{5}$$

The values of this ratio calculated along the catalyst bed, for particles with diameter in the range 50 - 250 μm (having an average dimension of 74.7 μm) are smaller than 0.01 on the entire working temperature and composition domain (Fig. 4). Consequently, the influence of the gas–solid mass transfer on the overall process kinetics can be neglected.

To check the heat transfer influence on process kinetics, we evaluated the internal and external temperature gradients of the catalyst pellet, according to the relations:

$$\Delta T_{int} = \frac{D_e \cdot (-\Delta H_{RA}) \cdot C_t\, y_{A,S}}{\lambda_e} \tag{6}$$

$$\Delta T_{ext} = \frac{k_G \cdot (-\Delta H_{RA}) \cdot C_t\, (y_A - y_{A,S})}{\alpha} \tag{7}$$

The solid–gas heat transfer coefficient, α, was calculated from the correlation proposed by Whitaker:[22]

$$Nu = \frac{1-\varepsilon}{\varepsilon}\left[\frac{1}{2}\left(\frac{Re_p}{1-\varepsilon}\right)^{0.5} + 0.2\left(\frac{Re_p}{1-\varepsilon}\right)^{2/3}\right] Pr^{1/3} \tag{8}$$

The values of effective diffusion coefficient for methane inside the porous pellet were obtained assuming that molecular and Knudsen mechanisms are predominant. The following relations were used in this aim:[19]

$$D_e = \frac{\varepsilon_g}{\tau}\cdot \overline{D}_A\,;\quad \frac{1}{\overline{D}_A} = \frac{1}{D_A} + \frac{1}{D_{K,A}}\,;\quad D_{K,A} = \frac{4}{3}\cdot \overline{r_p}\cdot\left(\frac{2}{\pi}\cdot\frac{R_G\cdot T}{M_A}\right)^{0.5} \tag{9}$$

with the molecular diffusion coefficient of methane, D_A calculated using the equation proposed by Reid *et al.*[23] and $\overline{r_p}$ = 10^{-8}m according to Zanfir and Gavriilidis.[24] The variation of enthalpy in the combustion reaction was calculated by the well known Hess and Kirchoff equations, using data published by Reid *et al.*[23] For the thermal conductivity of the pellet we used the value 0.4 W/(m·K) recommended by Zanfir and Gavriilidis.[24]

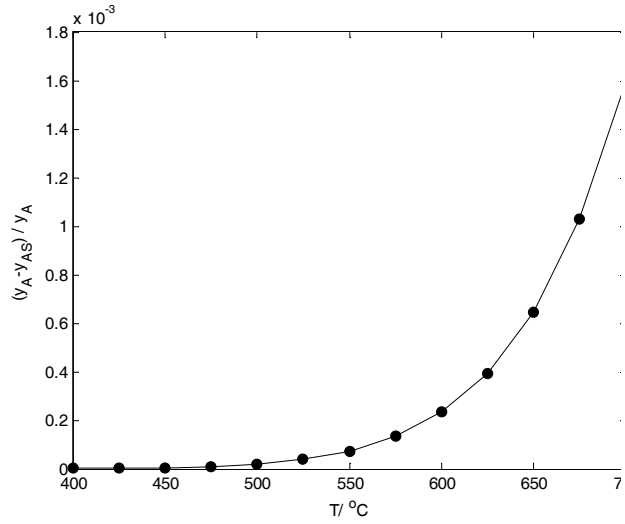

Fig. 4 – Temperature dependence of external concentration gradient.

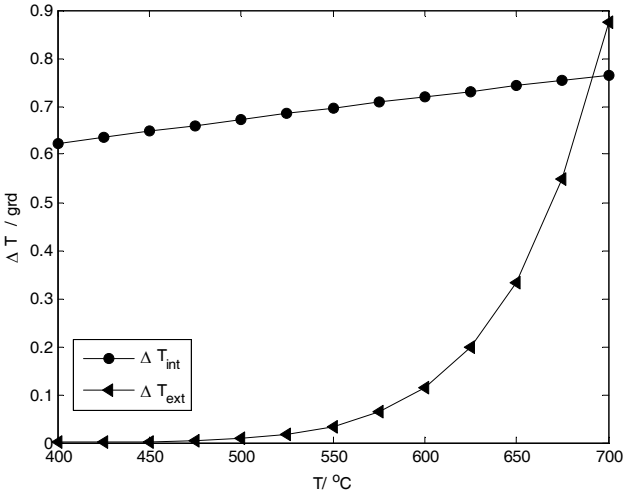

Fig. 5 – Temperature dependence of internal, respectively external temperature gradient.

(feed methane concentration 1.2 mol%; space velocity, 45000 $cm^3/(g_{cat}\ h)$)

The calculated internal and external temperature gradients are given as function of gas phase temperature in Fig. 5. As seen, the values are smaller than 1 K for all the working range, at the limit of significance, considering the accuracy of the published relations and values used in the calculus. Therefore, we neglected the influence of temperature gradients in the calculus, assuming the catalyst pellet isothermal at the temperature of the flowing gas.

Surface reaction kinetics

Several kinetic expressions, for methane combustion on precious metals catalysts, were published by different authors.[8, 17, 18, 26–28] In the present paper we have tested the models based on Langmuir-Hinshelwood (LH) or Eley-Rideal (ER) mechanisms assuming surface reaction between adsorbed or gaseous methane and adsorbed oxygen (non-dissociated or dissociated) corresponding to expressions (10)-(13):

LH non-dissociated oxygen adsorption[15]

$$v_{RA} = k_r \frac{K_A p_A K_O p_O}{(1 + K_A p_A + K_O p_O)^2} \quad (10)$$

LH dissociated oxygen adsorption [14-16]

$$v_{RA} = k_r \frac{K_A p_A (K_O p_O)^{0.5}}{(1 + K_A p_A + (K_O p_O)^{0.5})^2} \quad (11)$$

ER non-dissociated oxygen adsorption [15, 16]

$$v_{RA} = k_r \frac{p_A K_O p_O}{1 + K_O p_O} \quad (12)$$

ER dissociated oxygen adsorption [15, 16]

$$v_{RA} = k_r \frac{p_A (K_O p_O)^{0.5}}{1 + (K_O p_O)^{0.5}} \quad (13)$$

As our experiments were carried out in high oxygen excess, the oxygen concentration is practically constant along the catalyst bed and the rate equation (10)-(13) can be simplified to a pseudo-first order expression with respect to methane:

$$v_{RA} = k_m p_A; \quad k_m = k_{m0} \exp\left(-E_a/(R \cdot T)\right) \quad (14)$$

Several authors tested a general power law expression:

$$v_{RA} = k_m p_A^m p_O^n \quad (15)$$

However, the majority of these are reporting reaction order values m close to unity and n close to zero (see Table 3).

Table 3

Parameter values in power-law rate expressions (15) for methane combustion on Pt/Al_2O_3

Reference	E_a (kcal/mol)	k_0	m	n
Present work	33.5	$9.153 \cdot 10^4$ ($kmol/(kg_{cat} \cdot s \cdot bar^{m+n})$)	1	0.0
Anderson et al. [29]	23.5 (0.5 % wt.)	$2.24 \cdot 10^7$ (1/s)	1.0	0.0
Firth and Holland [30]	47.8	-	1.0	0.0
Yao [31]	21 (wire) 24 (Al_2O_3)	- -	1.0 1.2	- 0.6 - 0.6
Trimm and Lam [16]	20.6 (T>813 K) 44.7 (T<813 K)	- -	1.0 1.0	1.0 0.75
Niwa et al. [32]	25.2 (0.5 % wt.)	-	0.9	0.0
Cullis and Willatt [33]	5.78 (T>630 K) 27.3 (T<630 K)	-	-	-
Arai et al.[18]	27.6 (1 % wt.)	-	T = 723 K 0.9 T = 923 K 1.1	- 0.5 - 0.3
Otto [34]	35.1 (0.41 % wt.)	-	1.0	0.0
Song et al.[35]	32.2	$1.3 \cdot 10^{11}$ ($cm^{2.5}/mol^{0.5}/s$)	1.0	0.5
Ma et al.[28]	21	$1.20 \cdot 10^4$ ($mol/m^2/h/kPa^{m+n}$)	0.95	- 0.17
Kolaczkowski and Serbetcioglu [36]	31.3	$2.84 \cdot 10^8$ ($mol/m^2/s$)	0.72	0.0
Veser and Schmidt [37]	26.3	-	-	-
Kuper et al.[38]	36	$1.78 \cdot 10^8$ ($mol/m^2/s$)	1.0	-
Aube and Sapoundjiev [39]	13	$1.35 \cdot 10^4$ (1/s)	1.0	0.0
Garetto and Apesteguia [40, 41]	17	-	1.0	0.0
Fullerton et al.[42]	22	$1 \cdot 10^8$ (mL/s/g)	1.0	0.0

We obtained a reasonable good concordance of the first order expression (14) to our experimental data (measured on catalyst grain dimensions between 50 and 250 μm), the estimated activation energy confirming previous published values (Table 3). The parameters k_{m0} and E_a appearing in the rate expression (14) were evaluated assuming a pseudo-homogeneous plug-flow model of the experimental reactor.[19] The contribution of axial mixing to the mass transport inside the catalyst bed was neglected, considering that the ratio of catalyst bed height to particle diameter is relatively high ($L/d_p > 150$).

The influences of the feed concentration of methane and gas flow rate respectively on the methane conversion are presented in Figs. 6 and 7. As seen, on the working domain, the most important dependence is observed in respect with the total gas flow rate, the influence of methane feed concentration being not significant, due to the relatively small interval we considered.

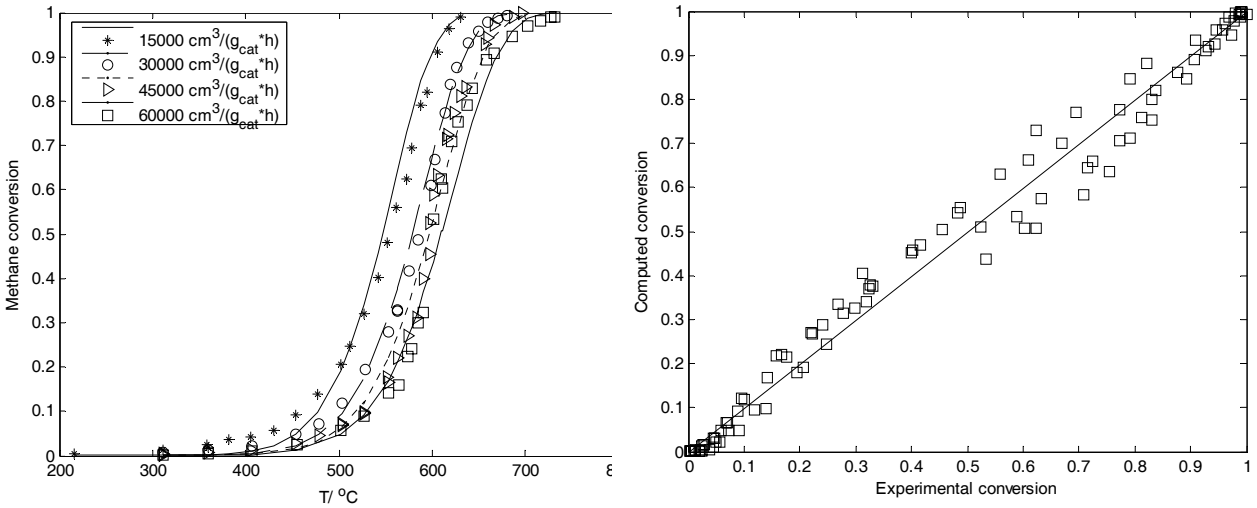

(a) (b)

Fig. 6 – (a) Combustion conversion-temperature curves for different feed total flow rates (feed methane concentration 1.2 % mol, catalyst size 50-250μm); the points represent measurements and the lines calculated values by kinetic model (14); (b) calculated versus experimental values of methane conversion (parity diagram).

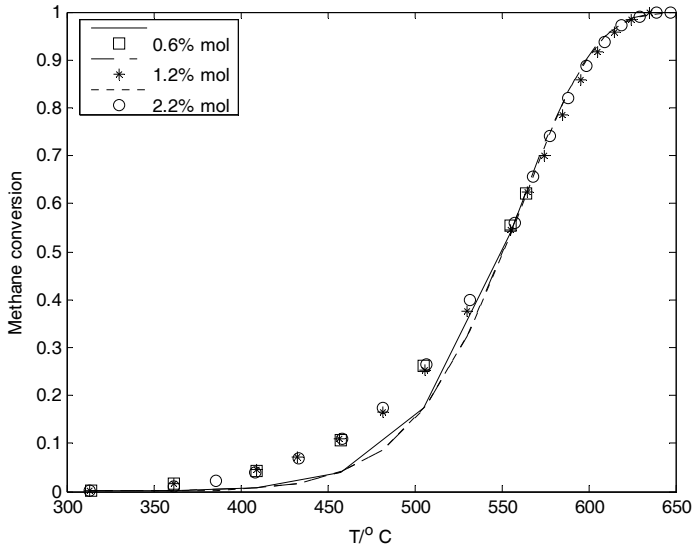

Fig. 7 – Combustion conversion-temperature curves for different methane feed concentrations (GHSV = 15000 $cm^3/(g_{cat}$ h), catalyst size 50-250μm); the points represent measurements and the lines calculated values by kinetic model (14).

As mentioned above, the kinetic parameters were evaluated from experimental data obtained on catalyst particle dimensions between 50 and 250 μm. For other particle dimensions, the influence of internal diffusion can be evaluated by the effectiveness factor using the relations:

$$\eta_i = \frac{1}{\varphi_m}\left(\frac{1}{tgh(3\cdot\varphi_m)} - \frac{1}{3\cdot\varphi_m}\right) \quad (16)$$

$$\varphi_m = \frac{d_p}{6}\sqrt{\frac{k_v}{D_e}};\ k_v = k_m RT\,\rho_{bed}/(1-\varepsilon) \quad (17)$$

Based on these relations we calculated the dependence of internal effectiveness factor on temperature for different catalyst particle dimensions we tested experimentally in Fig. 1, considering an averaged value of the pellet size. The results are presented in Fig. 8. As seen, for grain size higher than 250 μm, depending on the reaction temperature, the internal diffusion can influence in an important measure the process kinetics.

During our experiments, a continuous deactivation of the catalyst was observed, caused probably by the platinum sintering and oxidation to PtO_2 at high temperature and the volatilization of the oxide. This phenomenon was studied in a separate experiment, where we measured the evolution of methane conversion in respect with the on stream time of catalyst, keeping constant the reaction temperature, feed flow rate and inlet methane concentration. The results are presented in Fig. 9. As observed, the decrease of methane conversion is faster on first 25-30h of running. Onward, the time gradient of the methane conversion is lower, appearing a clear tendency of stabilization.

Defining the activity of the catalyst as the ratio of the current combustion rate to the combustion rate on the fresh catalyst, one obtains the expression:

$$v_{RA}(t) = a(t)\cdot v_{RA,0} \quad (18)$$

In the hypothesis of plug flow catalytic reactor and neglecting the variation of catalyst activity during a time interval equal to the residence time in the bed, the methane balance in the catalyst bed is expressed by the equation:

$$\frac{d\,X_A}{dm} = \frac{1}{D_{MA,0}}\cdot v_{RA} \quad (19)$$

Considering the methane conversion dependence of the combustion rate expression:

$$v_{RA} = \mathrm{a}\ k_m p_{A,0}(1-X_A) \quad (20)$$

and substituting in (19) one obtains by integration:

$$a(t) = \frac{D_{MA,0}}{k_m\cdot p_{A,0}\cdot m_c} ln\frac{1}{1-X_A(t)} \quad (21)$$

Assuming as 'fresh catalyst' the state of catalyst at t = 0, corresponding to the conversion $X_{A0} = 0.933$, one obtains:

$$a(t) = \frac{ln\left[1-X_A(t)\right]}{ln\left[1-X_{A0}\right]} \quad (22)$$

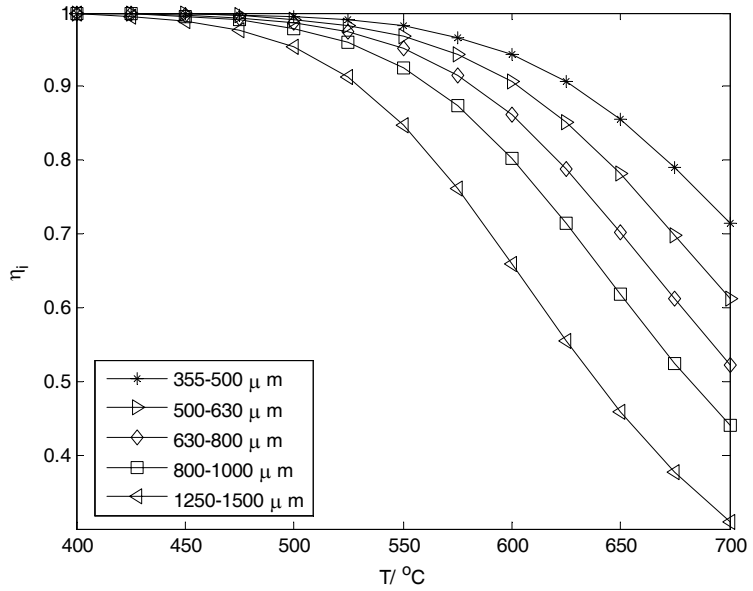

Fig. 8 – Calculated effectiveness factor (feed methane concentration 1.2 mol%; space velocity, 45000 $cm^3/(g_{cat}\ h)$).

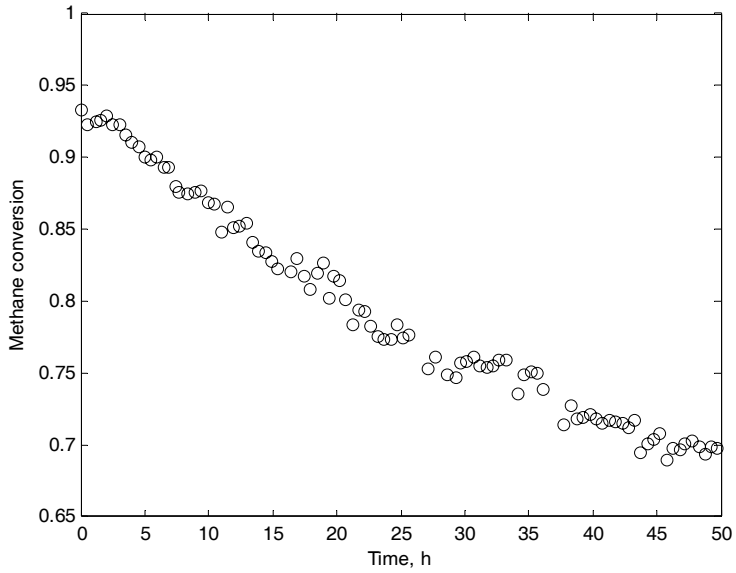

Fig. 9 – Methane conversion as a function of the time on stream (1.2 % CH_4 (mol), GHSV = 45000 $cm^3/(g_{cat}$ h), T = 605°C).

This relation permits to calculate the catalyst activity at each sampling time where is measured the methane conversion. The conversion values presented in Fig. 9 permit to build the activity–time curve shown in Fig. 10. As observed, in the first 50 hours of on stream time, the catalyst activity is approximately halved. However, on the following time interval the rate of deactivation becomes much smaller, appearing a trend of stabilization. The resulting time evolution of catalyst activity is presented by the points appearing in Fig. 10.

To represent quantitatively the time decrease of catalyst activity, we used the empirical power law decay rate:

$$\frac{da}{dt} = -k_d a^{\beta} \tag{23}$$

The parameter values of deactivation equation (23), obtained by fitting the experimental data presented in Fig. 10 are $k_d = 6.41 \cdot 10^{-4}$ min^{-1} and $\beta = 2.68$. This result is relatively closed to literature data that are evidencing a second order kinetics for the sintering deactivation mechanism.[43]

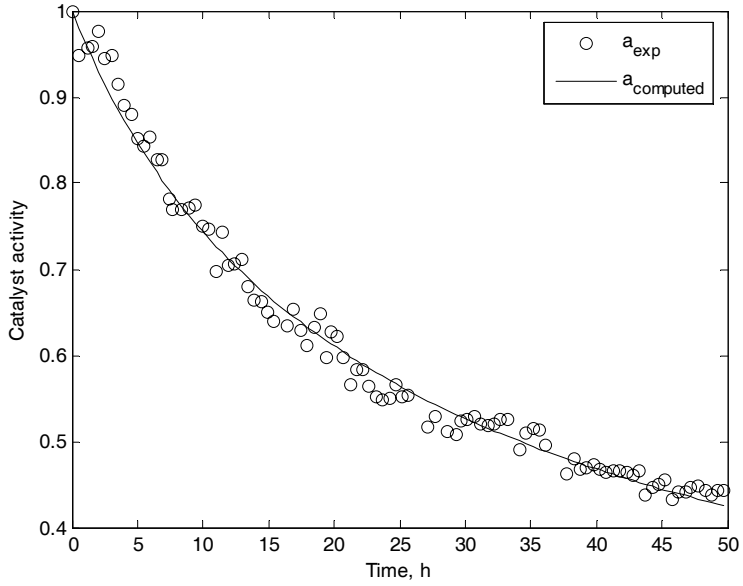

Fig. 10 – Catalyst activity as a function of on-stream time. The points represent experimental data and the line calculated values (1.2 mol % CH_4 ; GHSV = 45000 $cm^3/(g_{cat}$ h); T = 605°C).

CONCLUSIONS

In this work it was studied the kinetics of the combustion of lean methane mixtures with air over a commercial Pt/alumina catalyst (0.5 wt % Pt). The investigations of the process kinetics evidenced a good adequacy of the first order power law model to experimental data, this being explained by the high excess of oxygen in the reaction mixture. During the combustion experiments, it was observed a significant deactivation of the catalyst, particularly on first 25-30 hours of running. A deactivation experiment in isothermal conditions at 605 ^{o}C evidenced an approximately 50 % decrease of catalyst activity during the first 50 hours of exploitation. On the following time interval the rate of deactivation becomes much smaller, appearing a trend of stabilization. In order to represent the time dependence of catalyst activity we proposed a power law empirical relation that is fitting with a good accuracy the experimental data.

Nomenclature

a – catalyst activity, dimensionless
a_v – specific gas-solid surface area, $m^2_{GS}/m^3_{particle}$
C_A – molar concentration of methane, $kmol/m^3$
C_t – overall molar concentration of the gas phase, $kmol/m^3$
d_p – mean catalyst particle size, m
D_A – methane molecular diffusion coefficient, m^2/s
D_e – effective diffusion coefficient of methane in the porous catalyst particle, m^2/s
D_{KA} – methane Knudsen diffusion coefficient, m^2/s
D_{MA0} – feed methane flow rate, kmol/s
E_a – apparent activation energy of methane combustion process, kcal/mol
ΔH_{RA} – reaction enthalpy, J/kmol
j_D – Chilton-Colburn number for mass transfer, dimensionless
k_d – deactivation rate constant, 1/s
k_G – interphase mass transfer coefficient, m/s
k_m – combustion rate constant, kmol $kg^{-1}s^{-1}$ bar^{-1}
k_v – constant rate of catalytic reaction, s^{-1}
K_A, K_O – adsorption equilibrium constants of methane and oxygen respectively, bar^{-1}
m_c – mass of the catalyst, kg
M_A – molecular mass of methane, kg/kmol
N_A – methane flux transferred toward the external particle surface, kmol m^{-2} s^{-1}
p – total pressure, bar
p_{A0} – inlet methane partial pressure of methane, bar
p_A, p_O – methane and oxygen partial pressure, bar
$r_{A,S}$ – methane reaction rate $kmol \cdot m^{-3}_{bed} \cdot s^{-1}$
$\overline{r_p}$ – mean pores radius, m
R – universal gas constants; 0.082 m^3 bar $kmol^{-1}K^{-1}$
R_G – universal gas constants; 8310 J $kmol^{-1}K^{-1}$
Re_p – Reynolds number for catalyst particle, dimensionless
Sc – Schmidt number, dimensionless
t – on- stream time of the catalyst, s
T – working temperature, K
ΔT_{ext}, ΔT_{int} – external, respectively internal temperature gradient, K
u – superficial gas velocity, m/s
v_{RA} – methane reaction rate, $kmol/(kg_{cat} \cdot s)$
$v_{RA,0}$ – methane reaction rate at t = 0, $kmol/(kg_{cat} \cdot s)$
X_A – methane conversion
y_A, $y_{A,S}$ – mole fraction of methane in the flowing gas and on the external catalyst surface respectively
α – gas to solid heat transfer coefficient, $W/(m^2 \cdot K)$
ε – bed porosity, ε = 0.4 m^3_{gas}/m^3_{bed}
ε_g – catalyst particle porosity, ε_g = 0.5 $m^3_{gas}/m^3_{particle}$
η – gas dynamic viscosity, kg/(m s)
η_j – internal effectiveness factor, dimensionless
λ_e – effective heat conductivity of the catalyst particle, $W/(m \cdot K)$
ρ – gas density, kg/m^3
ρ_{bed} – catalyst density in the bed, kg_{cat}/m^3_{bed}
τ – tortuosity factor, τ = 4
ν_A – stoichiometric coefficient of methane
$\Delta\nu$ – variation in number of moles for the combustion reaction (considering the total oxidation to carbon dioxide)
φ_m – Thiele modulus

REFERENCES

1. G.W. Cordonna, M. Kosanovich and E. R. Becker, *Platinum Metals Rev.*, **1989**, *33*, 47-54.
2. H. Arai and M. Machida, *Catal. Today*, **1991**, *10*, 81-94.
3. G. Centi, *J. Molec. Catal. A: Chem.*, **2001**, *173*, 287-312.
4. C. Heneghan, G. Hutchings and S. Taylor, *SPR - Catalysis*, **2004**, *17*, 105-151.
5. J. J. Spivey, *Ind. Eng. Chem. Res.*, **1987**, *26*, 2165-2180.
6 J. J. Spivey, *SPR - Catalysis*, **1989**, *8*, 157-203.
7. S. R. Deshmukh and D. G. Vlachos, *Combust. Flame*, **2007,** *149,* 366-383.
8. S. T. Seyama, *Cat. Rev. – Sci. Eng.,* **1992,** *34*, 281-300.
9. J. Mantzaras, *Catal. Today*, **2006**, *117,* 394-406.
10. E. Becker, P.A. Carlsson, H. Gronbeck and M. Skoglundh, *J. Catal.,* **2007**, *252*, 11-17.
11. P. Gelin and M. Primet, *Appl. Catal.B*, **2002**, *39*, 1-37.
12. S. Oh, P. Mitchell and R. Siewert, *J. Catal.*, **1991**, *132*, 287-301.

13. R. Burch and P.K. Loader, *Appl. Catal. B*, **1994***, 5,* 149-164.
14. R. Burch, P.K. Loader and F.J. Urbano, *Catal. Today*, **1996**, *27*, 243-248.
15. R. Burch, D. Crittle and M. Hayes, *Catal. Today*, **1999**, *47,* 229-237.
16. D.L. Trimm and C.-W. Lam*, Chem. Eng. Sci.,* **1980,** *35*, 1405-1413.
17. L. Van de Beld, "Air Purification by Catalytic Oxidation in an Adiabatic Packed Bed Reactor with Periodic Flow Reversal", PhD Thesis, Netherlands, 1995.
18. H. Arai, T. Yamada, K. Eguchi and T. Seiyama, *Appl. Catal.*, **1986,** *26*, 265-276.
19. G.F. Froment and K. Bischoff, "Chemical Reactor Analysis and Design", John Wiley, New York, 1990.
20. R.B. Bird, E.S. Stewart and E.N. Lightfoot, "Transport Phenomena", John Wiley, New York, 1960.
21. F. Yoshida, D. Ramaswami and O.A. Hougen, *AIChE J.*, **1962,** *2*, 5-11.
22. S. Whitaker, *AIChE J.*, **1972**, *18*, 361-371.
23. C. Reid, J.M. Prausnitz and B.E. Poling, "The properties of gases and liquids", Mc Graw Hill, New York, 1987.
24. M. Zanfir and A. Gavriilidis, *Chem. Eng. Sci.,* **2003,** *58*, 3947-3960.
25. J.M. Smith, "Chemical Engineering Kinetics", Mc Graw Hill, New York, 1970**,** second ed.
26. G. Saracco, F. Geobaldo and G. Baldi, *Appl. Catal. B*, **1999**, *20,* 277-288.
27. R. Auer and F. Thyrion, *Ind. Eng. Chem. Res.,* **2002**, *41*, 680-690.
28. L. Ma, D.L. Trimm and C. Jiang, *Appl. Catal. A*, **1996**, *138*, 275-283.
29. R.B. Anderson, K.C.Stein, J.J.Fennan and L.J.E. Hofer, *Ind. Eng.Chem.***, 1961**, *53*, 809-812.
30. J.G. Firth and H.B. Holland, *Trans. Faraday Soc.*, **1969**, *65*, 1121-1127.
31. Y.-F.Y. Yao, *Ind. Eng. Chem. Prod. Res. Dev.*, **1980,** *19*, 293-298.
32. M. Niwa, K. Awano and Y. Murakami, *Appl. Catal.,* **1983**, *7*, 317-325.
33. C.F. Cullis and B.M. Willatt, *J. Catal.,* **1983,** *83*, 267-285.
34. K. Otto, *Langmuir*, **1989**, 5, 1364-1369.
35. X. Song, W.R.Wiliams, L.D.Schmidt and R.Aris, *Combust. Flame*, **1991,** *84*, 292-311.
36. S.T. Kolaczkowski and S. Serbetcioglu, *Appl. Catal. A*, **1996,** *138*, 199-214.
37. G. Veser and L. Schmidt, *AIChE J.*, **1996,** *42*, 1077-1087.
38. W.J. Kuper, M. Blaauw, F. van der Berg and G.H. Graaf, *Catal. Today*, **1999,** *47*, 377-389.
39. F. Aube and H. Sapoundjiev, *Comput. Chem Eng.*, **2000,** *24*, 2623-2632.
40. T.F.Garetto and C.R.Apesteguia, *Catal. Today*, **2000,** *62*, 189-199.
41. T.F.Garetto and C.R.Apesteguia, *Stud. Surf. Sci. Catal.*, **2000,** *130*, 575-580.
42. D.J. Fullerton, A.V.K. Westwood, R. Brydson, M.V. Twigg and J.M. Jones, *Catal. Today*, **2003,** *81*, 659-671.
43. J. B. Butt and E. E. Petersen, "Activation, Deactivation and Poisoning of Catalysts", Academic Press, New York, 1988, p. 198.